Exactly solvable fermion-boson mapping representations

Osvaldo Civitarese and Marta Reboiro
Department of Physics, University of La Plata, C.C. 67, La Plata, Argentina
(Received 18 November 1997; revised manuscript received 13 February 1998)

The Holstein-Primakoff boson mapping technique is applied to transform Hamiltonians defined in terms of the generators of the SU(2) and Sp(4) groups. These solvable models consist of a pair of fermions which interact with hard bosons. It is shown that the mapping to ideal bosons preserves the algebra and that exact matrix elements of the original fermionic Hamiltonian can be reconstructed from the bosonic representation. [S0556-2813(98)03006-4]

PACS number(s): 21.60.Fw, 21.60.Jz

I. INTRODUCTION

The development of microscopic nuclear models has been largely influenced by the findings of fermion-boson mapping techniques [1], particularly in the analysis of exactly solvable models and their extensions to realistic cases. Among these models, the ones based on the SU(2), Sp(4), SO(5), and SO(8) algebras have received considerable attention. Recently, results of the use of the SO(5) and SO(8) groups have been reported in the boson description of four fermion correlations [2]. Central to these studies is the formulation of exact solutions applicable to the treatment of nuclear short range correlations, like pairing [3] and isospin-pairing dependent effects [2]. Also, the study of nonperturbative schemes to describe interactions between fermions and bosons has some relevance in different situations where the usual perturbative expansion fails. This problem is found in the theory of strong interactions [4] and in the microscopic description of nuclear many-body systems and finite nuclei [5]. The description of these systems can be achieved by using boson expansion methods [6–9]. Among these methods one can select the boson expansion of Ref. [10], which is a mapping of bifermion operators onto boson operators. The method was originally introduced in [10] for the generators of SU(2) and it was lately generalized for the generators of Sp(4) by Evans and Krauss [11]. The representations are constructed by requiring that the algebra obeyed by bilinear operators in the transformed space be the same as in the original one.

It is the aim of this work to describe the application of this mapping to exactly solvable models where a pair of fermions interact with hard bosons. The first of these models, which shall be referred to as the SU(2) case, was proposed by Schütte and Da Providencia [12]. These authors have added to the Lipkin model [13] a bosonic degree of freedom. The second model, the Sp(4) case, is an extension of the one of [12] and it includes two additional external bosons. These bosons can interact with fermionic operators which create (annihilate) two-particle and two-hole states, respectively [14]. The introduction of these new degrees of freedom was motivated by the need to describe the interaction of dibaryons with hard bosons [15]. As described in [16], the Sp(4) algebra can accommodate particle, hole, and particle-hole pairs, both of collective and noncollective structure. Since exact solutions of the SU(2) model of [12] are known, the case will provide us with a testing ground for the boson mapping method, both analytically and numerically. The results for the other case, i.e., the model which exhibits the Sp(4) group structure, will be presented in an algebraic way to allow for numerical applications. The underlying physical motivations for both models are the analysis of symmetry breaking effects and the collapse of linear bosonizations for certain values of the interactions. These questions have received considerable attention in different fields, for instance in the study of the validity of the random phase approximation in elementary [17] and realistic [18] situations.

In the first part of the following section the algebra of the SU(2) and Sp(4) models is reviewed and the transformation onto boson variables is introduced. Next, the matrix elements of the fermion Hamiltonians are constructed in the boson space. Exact solutions and the solutions obtained by applying boson-mapping techniques are compared in the last part of the section, where relevant matrix elements are listed. Results corresponding to first excited states are discussed in the framework of the random phase approximation (RPA) and in the boson mapping representation, respectively. For the case of the SU(2) Hamiltonian, the results of the RPA are also available from studies on the validity of the use of perturbative expansions in the presence of spurious modes [17].

II. FORMALISM

In this section we shall introduce the generators of the SU(2) and Sp(4) groups, the corresponding symmetry operators, and the associated basis. We shall transform the fermionic Hamiltonians in terms of ideal bosons and compare exact solutions with the ones given by the mapping method. In dealing with the applications of the formalism we shall treat excitations in a restricted subspace, like the one of the random phase approximation [6].

A. The SU(2) case

We begin by applying the boson mapping of [10] to the Hamiltonian proposed by Schütte and Da Providencia [12]. The system consists of N fermions moving in two single shells (hereafter denoted by the subindexes 1 and 2). Each shell has 2Ω substates which are labeled by the quantum number k. The energy difference between shells is fixed by the scale ω_f. The creation and annihilation operators of particles belonging to the upper level, 2, are denoted by $a^\dagger_{2k}$ and

a_{2k}, respectively, while for holes in the lower level, 1, the creation and annihilation operators are denoted by $b^{\dagger}_{1k}$ and b_{1k}.

The fermions are coupled to an external boson field represented by the creation (annihilation) operators $B^{\dagger}$ (B) and by the energy ω_B, respectively.

The Hamiltonian reads [12]

$$H=\frac{\omega_f}{2}(\nu+\overline{\nu})+\omega_B B^{\dagger}B+G_1(T_+B^{\dagger}+T_-B). \quad (1)$$

G_1 is the strength of the interaction in the particle-hole channel and the operators

$$\nu=\sum_k a^{\dagger}_{2k}a_{2k}, \quad \overline{\nu}=\sum_k b^{\dagger}_{1k}b_{1k}, \quad (2)$$

are particle (ν) and hole ($\overline{\nu}$) number operators.

The operators $T_{\pm}$ and T_0 are the generators of the algebra of the group SU(2) [19]. In terms of bi-linear combinations of fermion operators these generators read

$$T_+=\sum_k a^{\dagger}_{2k}b^{\dagger}_{1k}, \quad T_-=(T_+)^{\dagger},$$

$$T_0=\frac{1}{2}(\nu+\overline{\nu})-\Omega. \quad (3)$$

The Hamiltonian (1) commutes with the operator

$$P=B^{\dagger}B-\frac{1}{2}(\nu+\overline{\nu}). \quad (4)$$

Therefore, the matrix elements of H can be calculated in a basis labeled by the eigenvalues of the number operators for bosons and fermions, as shown in [12]. The corresponding expressions are given in [12] and we shall avoid repeating them here.

Next we transform the original fermion space onto the boson space $\{b_f\}$, where $[b_f,b_f^{\dagger}]=1$, by preserving the original SU(2) commutation relations between the generators T_+, T_-, and T_0, i.e.,

$$T_+=b_f^{\dagger}(2\Omega-b_f^{\dagger}b_f)^{1/2}, \quad T_-=(2\Omega-b_f^{\dagger}b_f)^{1/2}b_f,$$

$$T_0=b_f^{\dagger}b_f-\Omega. \quad (5)$$

The new boson operator $b_f^{\dagger}$ and its Hermitian conjugate b_f are introduced, instead of the original ones $B^{\dagger}$ and B, because fermionic and bosonic excitations of the Hamiltonian (1) have, in general, different scales.

After performing the above transformations (for short, mapping) we get for the Holstein-Primakoff [10] image of the Hamiltonian (1) the expression

$$H_B=\omega_f\hat{n}_f+\omega_B\hat{N}_B+G_1[b_f^{\dagger}(2\Omega-b_f^{\dagger}b_f)B^{\dagger}+\text{H.c.}], \quad (6)$$

where we have defined the boson numbers $\hat{N}_B=B^{\dagger}B$ and $\hat{n}_f=b_f^{\dagger}b_f$.

We shall diagonalize H_B in the basis expanded by

$$|n_f n_b\rangle=\frac{1}{\sqrt{n_f!\,n_b!}}b_f^{\dagger n_f}B^{\dagger n_b}|\rangle. \quad (7)$$

The nonzero matrix elements of H_B are

$$\langle n_f n_b|H_B|n_f n_b\rangle=\omega_f n_f+\omega_B n_b,$$

$$\langle n_f+1\,n_b+1|H_B|n_f n_b\rangle=G_1[(n_f+1)(n_b+1)(2\Omega-n_f)]^{1/2}. \quad (8)$$

The operator P, of Eq. (4), can be mapped onto the operator

$$P_B=\hat{N}_B-\hat{n}_f, \quad (9)$$

leading to the identity

$$P_B|n_f n_b\rangle=L|n_f n_b\rangle (L=n_b-n_f). \quad (10)$$

The basis (7) can also be labeled by the eigenvalues of P_B, hereafter denoted by L. By using this notation, the matrix elements (8) can be written

$$\langle L,n_f|H_B|L,n_f\rangle=\omega_f n_f+\omega_B(n_f+L),$$

$$\langle L,n_f+1|H_B|L,n_f\rangle=G_1[(n_f+1)(n_f+1+L)(2\Omega-n_f)]^{1/2}. \quad (11)$$

These matrix elements, given by the Holstein-Primakoff boson mapping, coincide with the exact matrix elements, as can be seen from [12]. Exact solutions of this model have been obtained by a separation of variables followed by a perturbative expansion in terms of intrinsic and collective coordinates [17]. In the framework of the RPA method, the spectrum of excited states of Eq. (1), written in terms of phonon operators which are linear superpositions of fermion pairs and bosons, contains spuriosities which are not present in the exact solution. In this respect the boson mapping (5) belongs to the group of techniques which can be used to disentangle physical and spurious effects in approximate treatments of the Hamiltonian. In the next section we shall present RPA and exact results, obtained by using the boson mapping, in a regime of parameters of Eq. (1) where a transition from normal to deformed solutions [12] can be produced. As shown in [17] the separation of spurious and physical degrees of freedom is essential in this SU(2) model, if the RPA approximation is used to construct effective boson excitations.

B. The Sp(4) case

Bifermion excitations, of particle-particle, hole-hole, and particle-hole nature, were considered by Geyer and Hahne [16] in algebraic models. These models can be adopted, with some modifications, as the basic structures to represent scalar and vector couplings between bosons and fermions and they

can provide us with testing grounds for nonperturbative approaches [7]. As a generalization of the model of [12] we shall introduce the coupling of bifermion excitations with bosons. The fermionic degrees of freedom will be defined as in [16] while bosonic excitations will be represented by external bosons with particle-hole, particle-particle, and hole-hole contents, as done in the model of [12] for a single boson. Starting from these assumptions on the Hamiltonian we shall present the results of the boson mapping and show the elements of the basis and the resulting matrix elements. We have also performed numerical applications of the formalism and we shall comment on them, in the next section. Details related to the construction of the algebraic solution can be found in [11] and in [20].

We consider the Hamiltonian

$$H=H_{0f}+H_{0b}+H_{ph}+H_{pp}+H_{hh},$$

with

$$H_{0f}=\frac{\omega_f}{2}(\nu+\overline{\nu}),$$

$$H_{0b}=\omega_B B^\dagger B+\omega_p B_p^\dagger B_p+\omega_h B_h^\dagger B_h,$$

$$H_{ph}=G_1(T_+B^\dagger+T_-B),$$

$$H_{pp}=G_2(L_+B_h^\dagger+L_-B_h),$$

$$H_{hh}=G_3(K_+B_p^\dagger+K_-B_p). \tag{12}$$

In the above equation the fermions are coupled to bosons. These bosons are created by the operators $B^\dagger$, $B_p^\dagger$, and $B_h^\dagger$ and their energies are ω_B, ω_p, and ω_h, respectively. G_1 is, as in the previous example, the strength of the interaction in the particle-hole channel and G_2 and G_3 are the strengths of particle-particle and hole-hole channels.

The operators $T_\pm$, $L_\pm$, $K_\pm$, $S_\pm$, L_0, and K_0, of Eq. (12) are defined by

$$T_+=\sum_k a_{2k}^\dagger b_{1k}^\dagger, \quad T_-=(T_+)^\dagger,$$

$$T_0=L_0+K_0,$$

$$L_+=\sum_{k>0} a_{2k}^\dagger a_{2-k}^\dagger, \quad L_-=(L_+)^\dagger,$$

$$L_0=\frac{1}{2}(\nu-\Omega),$$

$$K_+=\sum_{k>0} b_{1k}^\dagger b_{1-k}^\dagger, \quad K_-=(K_+)^\dagger,$$

$$K_0=\frac{1}{2}(\overline{\nu}-\Omega),$$

$$S_+=\sum_k sg(k)a_{2-k}^\dagger b_{1k}, \quad S_-=(S_+)^\dagger,$$

$$S_0=L_0-K_0, \tag{13}$$

and they are the generators of the algebra of the simplectic group Sp(4) [16].

Exact solutions of this Hamiltonian can be obtained by group theoretical methods (see, please, [11,20] for details). The eigenvectors belong to the basis of the operators

$$P=B^\dagger B+B_p^\dagger B_p+B_h^\dagger B_h-\frac{1}{2}(\nu+\overline{\nu}),$$

$$R=B_h^\dagger B_h-B_p^\dagger B_p+\frac{1}{2}(\overline{\nu}-\nu). \tag{14}$$

In correspondence with the notation introduced after Eq. (6) we shall define the fermionic and bosonic number operators $\hat{n}_f=b_f^\dagger b_f$, $\hat{n}_p=b_p^\dagger b_p$, $\hat{n}_h=b_h^\dagger b_h$, $\hat{N}_B=B^\dagger B$, $\hat{N}_p=B_p^\dagger B_p$, and $\hat{N}_h=B_h^\dagger B_h$.

The boson mapping proposed in Ref. [11], preserves the algebra of the generators of this group. The corresponding boson images are

$$L_+=b_p^\dagger(\Omega-\hat{n}_p-\hat{n}_f)^{1/2}, \quad L_-=(L_+)^\dagger,$$

$$L_0=\left(\hat{n}_p+\frac{1}{2}\hat{n}_f-\frac{1}{2}\Omega\right),$$

$$K_+=b_h^\dagger(\Omega-\hat{n}_h-\hat{n}_f)^{1/2}, \quad K_-=(K_+)^\dagger,$$

$$K_0=\left(\hat{n}_h+\frac{1}{2}\hat{n}_f-\frac{1}{2}\Omega\right),$$

$$S_+=b_f^\dagger\Phi(\hat{n}_f)(\Omega-\hat{n}_p-\hat{n}_f)^{1/2}b_h - b_p^\dagger(\Omega-\hat{n}_h-\hat{n}_f)^{1/2}\Phi(\hat{n}_f)b_f,$$

$$S_-=(S_+)^\dagger,$$

$$T_+=-b_f^\dagger(\Omega-\hat{n}_h-\hat{n}_f)^{1/2}(\Omega-\hat{n}_p-\hat{n}_f)^{1/2}\Phi(\hat{n}_f) + \Phi(\hat{n}_f)b_p^\dagger b_h^\dagger b_f,$$

$$T_-=(T_+)^\dagger. \tag{15}$$

With these generators the mapped Hamiltonian reads

$$\begin{aligned}H_B=&\omega_f(\hat{n}_f+\hat{n}_p+\hat{n}_h)+\omega_B\hat{N}_B+\omega_p\hat{N}_p+\omega_h\hat{N}_h\\&+G_2[b_p^\dagger(\Omega-\hat{n}_p-\hat{n}_f)^{1/2}B_h^\dagger+\text{H.c.}]\\&+G_3[b_h^\dagger(\Omega-\hat{n}_h-\hat{n}_f)^{1/2}B_p^\dagger+\text{H.c.}]\\&+G_1[-b_f^\dagger(\Omega-\hat{n}_h-\hat{n}_f)^{1/2}(\Omega-\hat{n}_p-\hat{n}_f)^{1/2}\Phi(\hat{n}_f)B^\dagger\end{aligned}$$

$$+\Phi(\hat{n}_f)b_p^\dagger b_h^\dagger b_f B^\dagger + \text{H.c.}], \tag{16}$$

with

$$\Phi(\hat{n}_f)=\left[\frac{(2\Omega+2-\hat{n}_f)}{(\Omega+1-\hat{n}_f)(\Omega-\hat{n}_f)}\right]^{1/2}.$$

The images of the operators P and R, of Eq. (14), read

$$P_B=(\hat{N}_B+\hat{N}_p+\hat{N}_h)-(\hat{n}_f+\hat{n}_p+\hat{n}_h),$$

$$R_B=(\hat{N}_h+\hat{n}_h)-(\hat{N}_p+\hat{n}_p), \tag{17}$$

and the basis in the image space is defined by the eigenvectors

$$|\Phi^{\alpha\beta}_{N,L,k,m}\rangle = N^{\alpha\beta}_{N,L,k,m} b_f^{\dagger k} b_p^{\dagger m} b_h^{\dagger(2\Omega-N+m)} B^{\dagger(k+L)} \times B_p^{\dagger[(\alpha+\beta-L)/2+m]} B_h^{\dagger[(\alpha-\beta-L)/2+2\Omega-N+m]}|\rangle, \tag{18}$$

where $k=n_f$ and $m=n_p$. These states are labeled by the quantum numbers α and β and by the number of particles N. These quantum numbers are defined by

$$\alpha=N_B-n_f+N_p-n_p+N_h-n_h,$$

$$\beta=N_h+n_h-(N_p+n_p),$$

$$N=2\Omega-n_h+n_p. \tag{19}$$

In addition, we shall define $L=N_B-n_f$. After some algebra we have obtained the following nonzero matrix elements of H_B (16) in the basis (18)

$$\langle\Phi^{\alpha\beta}_{N,L,k,m}|H|\Phi^{\alpha\beta}_{N,L,k,m}\rangle=\omega_f(m+\Omega-N/2+m+k)+\omega_B(L+k)+\omega_p[\Omega-N/2+m+(\alpha-\beta-L)/2]+\omega_h[m+(\alpha+\beta-L)/2],$$

$$\langle\Phi^{\alpha\beta}_{N+2,L,k,m+1}|H|\Phi^{\alpha\beta}_{N,L,k,m}\rangle=G_2\sqrt{(m+1)\left(m+1+\frac{\alpha+\beta-L}{2}\right)(\Omega-k-m)},$$

$$\langle\Phi^{\alpha\beta}_{N+2,L,k,m}|H|\Phi^{\alpha\beta}_{N,L,k,m}\rangle=G_3\sqrt{\left(\Omega-\frac{N}{2}+m+1\right)}\sqrt{\left(\Omega-\frac{N}{2}+m+1+\frac{\alpha-\beta-L}{2}\right)\left(\frac{N}{2}-k-m\right)},$$

$$\langle\Phi^{\alpha\beta}_{N,L,k+1,m}|H|\Phi^{\alpha\beta}_{N,L,k,m}\rangle=-G_1\sqrt{(k+1)(k+1+L)}\sqrt{\frac{(2\Omega+2-k)(\Omega-m-k)[(N/2)-m-k]}{(\Omega+1-k)(\Omega-k)}},$$

$$\langle\Phi^{\alpha\beta}_{N,L+2,k-1,m+1}|H|\Phi^{\alpha\beta}_{N,L,k,m}\rangle=G_1\sqrt{k(m+1)}\sqrt{\frac{(\Omega-N/2+m+1)(L+k+1)(2\Omega+3-k)}{(\Omega-k+1)(\Omega+2-k)}}. \tag{20}$$

The complete set of nonzero matrix elements can be obtained from the above equations by observing the selection rules $N,k,m\rightarrow N\pm 2,k\pm 1,m\pm 1$.

In analogy to the case of the SU(2) model we observe that the matrix elements obtained in the image space and the exact ones, of the initial fermion and boson basis, do coincide. For a comparison between both sets of expressions, the reader is kindly referred to [20] where the exact matrix elements are listed.

III. RESULTS AND DISCUSSION

In the first part of this section we shall present the results obtained by applying the boson mapping introduced in the previous section to the SU(2) model of Ref. [12]. We aim at the comparison between the present results and the ones of [12] to assess the validity of the boson mapping. In order to remind the reader about the model of [12] we shall briefly summarize the conclusions of [12] concerning the structure of the exact ground state and excited states in the so-called normal and deformed phases. In the normal phase the absolute ground-state energy has $L=0$, which is the eigenvalue of the symmetry P corresponding to the unperturbed ground state. In this phase the number of fermion pairs and the number of bosons are the same. This regime persists for small values of G_1. For large values of G_1 the model of [12] exhibits a boson condensation, i.e., positive values of L are assigned to the absolute ground state. This is the so-called deformed phase. For values of ω_B larger than ω_f and for intermediate values of G_1 the model shows minima for values of $L<0$, i.e., a condensate of fermion pairs. We have verified that the results given by the boson mapping procedure coincide with the results of [12]. The absolute value of the ground-state energy, obtained in the boson mapping, is shown in Table I, with the corresponding values of the exact symmetry L and the one corresponding to the mean field approximation of H (see [17]). These results coincide with

TABLE I. Absolute ground-state energy, $E_L^{(\mathrm{g.s.})}$, as a function of the coupling constant $x=G_1\sqrt{2\Omega/\omega_f\omega_B}$, and the exact ($L$) and mean field ($L_{\mathrm{m.f.}}$) values of the symmetry P [Eq. (9)] defined in Eq. (10). Top and bottom correspond to $\omega_f=\omega_B=1$ and $\omega_f=1,\omega_B=3$, respectively.

x	$E_L^{(\mathrm{g.s.})}$	L	$L_{\mathrm{m.f.}}$
0.0	0.00	0	0.0
0.5	−0.13	0	0.0
1.0	−0.74	0	0.0
1.5	−5.83	5	5.2
2.0	−17.40	16	16.8
2.5	−33.60	33	33.1
3.0	−53.86	53	53.3
0.0	0.00	0	0.0
0.5	−0.20	0	0.0
1.0	−0.96	0	0.0
1.5	−6.43	−3	−3.8
2.0	−18.20	−2	−1.9
2.5	−34.50	3	2.6
3.0	−54.80	9	8.9

the results of Tables 1 and 3 of Ref. [12]. Also, one can see that the structure of the different phases found in [12] is preserved by the mapping. The parameters used in the calculations are given in the caption to Table I and they have been obtained for $N=2\Omega=30$ particles and the reduced coupling constant x is defined by $x=G_1\sqrt{2\Omega/\omega_f\omega_B}$. The dependence of the results upon the ratio between the unperturbed fermion and boson energies (ω_f and ω_B, respectively) is shown in Table I ($\omega_f=\omega_B=1$), ($\omega_f=1$, $\omega_B=3$). The results of Table I show the appearance of a fermion condensate ($L<0$), as is discussed in [12].

Figure 1 shows the values of the excitation energy corresponding to the first excited state of H (6), for different values of the coupling constant x and for positive and negative values of L. The spreading of the results corresponding to positive values of L is larger than the spreading associated to negative values of L, as can be seen from the results of Fig. 1.

The dependence of the first two eigenvalues, for different values of the coupling constant x and for $L=0,\pm1$, is shown in Fig. 2. For the case of $\omega_f=\omega_B=1$ [case (a)] the structure of the ground state is always given by positive values of L (see also Table I) and the transition from the normal to the deformed phase appears around the value $x=1$. The results for the negative value of L are always larger than the results for positive values and the energy of the first $L=1$ state is always smaller than the energy of the second $L=0$ state. A different behavior is shown by the curves of Fig. 2(b), where the second $L=0$ eigenstate and the first $L=1$ state become nearly degenerate around $x=1$ and a fermion condensate appears around $x=1.5$. This shows the strong dependence of the results upon the scale adopted for the bare energies, as is the case for the results of [12].

The results shown in Fig. 3 correspond to excitation energies obtained by using the RPA method (dashed lines) [12,17]. The results shown as exact results in Fig. 3 (solid

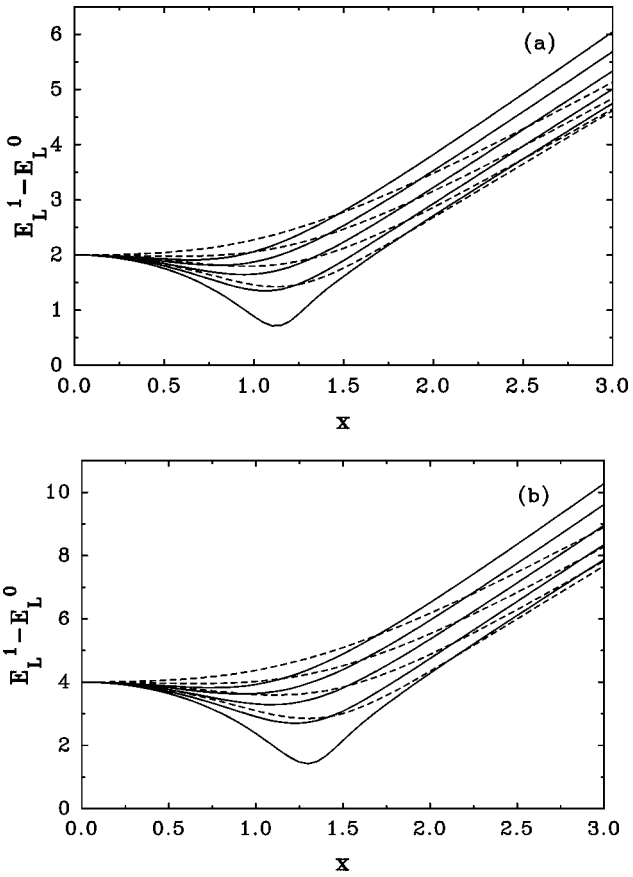

FIG. 1. Exact first excited states of Eq. (6) in the basis (7). Solid and dashed lines correspond to positive and negative values of L of Eq. (10), respectively. The results are shown for values of the coupling constant $x=G_1\sqrt{2\Omega/\omega_f\omega_B}$ in the interval $0\leqslant x\leqslant 3$ and for $N=2\Omega$ particles. The curves, from bottom to top, correspond to $L=0,4,8,12,16$ (solid lines) and $L=-4,-8,-12,-16$ (dashed lines). The upper box (a) shows results for $\omega_f=\omega_B=1$ and the lower box (b) shows results for the case with $\omega_f=1$, $\omega_B=3$.

lines) correspond to normal ($x\leqslant 1$) and deformed ($x>1$) solutions.

In the normal phase the absolute ground state has $L=0$ and the RPA values reproduce fairly well the exact energy difference between the first $L=1$ state and the ground state. Of the two solutions of Eq. (21) the value with the positive sign in front of the square root corresponds to $L=1$ and the absolute value of the other solution to $L=-1$, as in [12] and [17].

In the deformed phase the agreement between the RPA and exact results is evident for large values of x. Here, the exact energy of the first excited state is defined as the energy difference between the first two eigenvalues corresponding to the value of L which minimizes the absolute ground-state energy.

For the case of the deformed phase the RPA gives two solutions, one of them spurious and another which approaches the exact value. Around $x=1$ the RPA collapses. The RPA spurious mode also has zero energy and it is independent of the value used for the coupling constant x. The collapse of the first excited RPA state at $x=1$ signals the beginning of the deformed phase. The RPA values depend also upon the ratio of the fermionic and bosonic scales of the

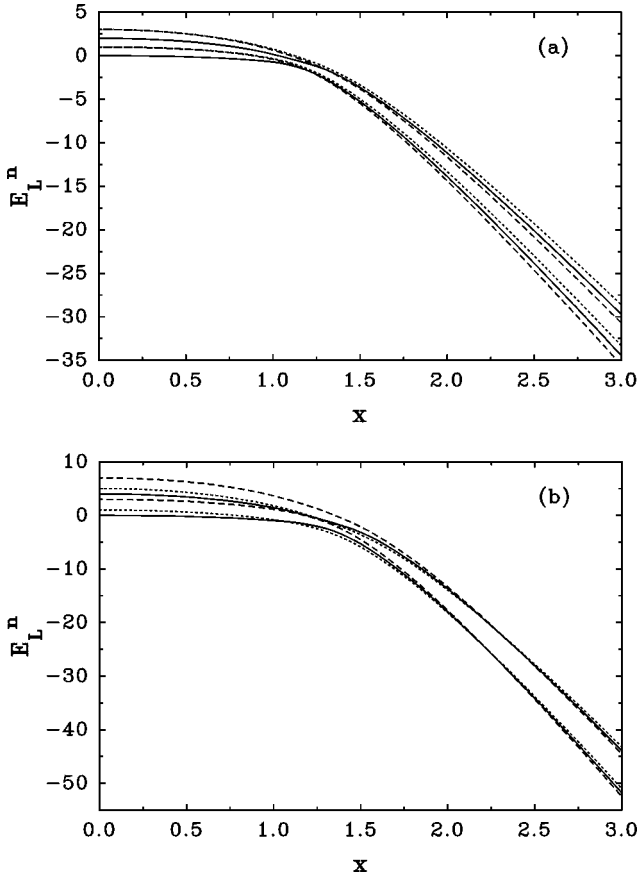

FIG. 2. Exact eigenstates of H (6) in the basis (7), for $L=\pm 1$ and $L=0$. Solid, dashed, and dotted lines read for the first two eigenvalues corresponding to $L=0,1,-1$, respectively. The results correspond to the parameters given in Fig. 1 for the upper and lower boxes (a) and (b).

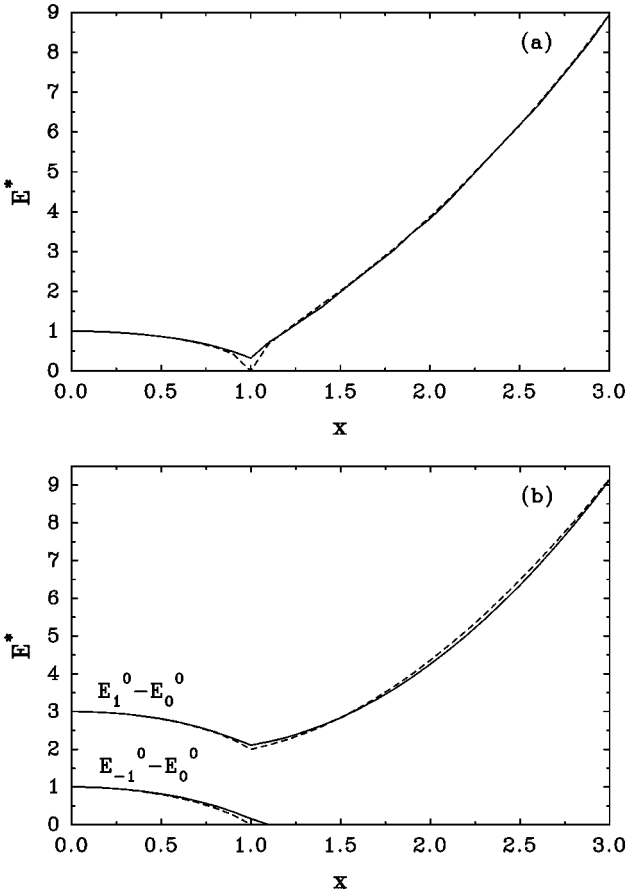

FIG. 3. Comparison between exact (solid line) and RPA (dashed line) results for the energy of the first excited state of Eq. (6). The upper (a) and lower (b) boxes show results obtained with the parameters defined in Fig. 1.

Hamiltonian. This is shown by the comparison between cases (a) and (b) of Fig. 3. The effect produced by the asymmetry ($\omega_f \neq \omega_B$) upon the RPA eigenvalue is shown by the lower curve of Fig. 3(b). The RPA expression of the first excited state, in the normal phase, is the following:

$$\omega_{\mathrm{RPA}}=\frac{1}{2}|\omega_f-\omega_B|\pm\frac{1}{2}(\omega_f+\omega_B)\sqrt{1-\left(\frac{2G_1\sqrt{2\Omega}}{\omega_f+\omega_B}\right)^2}. \tag{21}$$

For the deformed case ($x>1$) the RPA method yields

$$\omega_{\mathrm{RPA}}=\sqrt{\frac{(G_1\sqrt{2\Omega})^4}{\omega_B{}^2}+\omega_B^2-2\omega_f\omega_B}. \tag{22}$$

As said before, the RPA also gives a spurious solution at $\omega_{\mathrm{RPA}}=0$ [17]. The RPA solution of the previous equation can be compared with $E^1_{L,\min}-E^0_{L,\min}$ of the exact solution [12].

After this comparison between the solutions obtained with the methods of [12] and the present one, and to conclude with the first part of the discussions, it would be enough to say that we have shown that the use of the boson mapping method leads to a good agreement with the exact and approximate (RPA) solutions of the SU(2) model.

We can now discuss some of the features extracted from the numerical solutions of the Hamiltonian (16).

In the applications which we have performed, the matrix elements of Eq. (20) were calculated for $N=8$, $\Omega=4$ and all the energies w of Eq. (12) were fixed at the value $w=1$. The coupling constants G_i of Eq. (12) were transformed into adimensional couplings x_i as in [12], i.e., by scaling the couplings with factors proportional to the inverse of the energies w_i. The values of x_i were varied in a mesh with steps of 0.25 and the Hamiltonian matrix (20) was diagonalized in a basis of states having good values of α and β, Eq. (19). For each set of values of the couplings x_i the spectrum of eigenvalues of H was obtained and optimal values of α and β were selected by searching for the lowest ground-state energy.

The solutions of the Sp(4) Hamiltonian also display a normal and a deformed regime, similar to the case of the SU(2) symmetry. We shall identify these normal and deformed phases in terms of the symmetry numbers α and β, which are the eigenvalues of Eq. (14). For interaction channels with couplings $x_i \leqslant 1$ ($i=$particle-particle, hole-hole, and particle-hole) the minima correspond to values of α and β close to zero (the normal phase). For larger values of x_i a condensate, of either fermion or boson origin, can be produced. The associated minima correspond to nonzero values of α, while β

can remain close to zero. As in the case of the model of [12] condensates in the Sp(4) model can correspond to positive or negative values of α. Positive values of α are associated to a condensate of bosons while negative values of α represent a condensate of fermions. The occurrence of such condensates is also a function of the fermionic and bosonic scales introduced in the Hamiltonian. For the Sp(4) Hamiltonian (16) the collapse of the RPA signals the splitting of the RPA phonons into phonons which are predominantly given by two-fermion components (particle-particle or hole-hole phonons) [18].

IV. SUMMARY AND OUTLOOK

The mapping of fermionic and bosonic degrees of freedom onto an ideal bosonic space has been performed for two Hamiltonians described by generators of the SU(2) and Sp(4) groups. It is shown that the mapping preserves the algebra. Also, it is found that the matrix elements of each of the Hamiltonians calculated in basis having exact symmetries coincide with the matrix elements obtained after applying the mapping onto the ideal boson space.

It is concluded that the mapping is a good alternative way to get exact solutions and that it may be easier to apply, instead of the algebraic way, in evaluating the validity of approximate methods, like the RPA. Applications of the mapping method to QCD inspired models are in progress [21].

ACKNOWLEDGMENTS

The authors are grateful for the financial support of CONICET, Argentina. This work is part of the project PMT-PICT0079 of the ANPCYT (Argentina).

[1] A. Klein and E. R. Marshalek, Rev. Mod. Phys. **63**, 375 (1991).
[2] J. Dobes and S. Pittel, nucl-th/9710053, 1997.
[3] O. Civitarese and M. Reboiro, Phys. Rev. C **56**, 1179 (1997); O. Civitarese, M. Reboiro, and P. Vogel, *ibid.* **56**, 1840 (1997).
[4] E. Leader and E. Predazzi, *Gauge Theories and New Physics* (Cambridge University Press, London, 1983).
[5] D. R. Bes and J. Kurchan, *The Treatment of Collective Coordinates in Many-body Systems*, Lecture Notes in Physics Vol. 34 (World Scientific, Singapore, 1990).
[6] P. Ring and P. Shuck, *The Nuclear Many-body Problem* (Springer, New York, 1980).
[7] P. O. Hess and J. C. Lopez, Nucl. Phys. **B30**, 936 (1993); P. O. Hess and D. Schütte, Ann. Phys. (N.Y.) **211**, 112 (1991).
[8] F. J. Dyson, Phys. Rev. **102**, 1217 (1956).
[9] S. V. Maleev, Sov. Phys. JETP **6**, 776 (1958).
[10] T. Holstein and H. Primakoff, Phys. Rev. **58**, 1098 (1940).
[11] J. A. Evans and N. Kraus, Phys. Lett. **37B**, 455 (1971).
[12] D. Schütte and J. Da Providencia, Nucl. Phys. **A282**, 518 (1977).
[13] H. J. Lipkin *et al.*, Nucl. Phys. **62**, 188 (1965).
[14] O. Civitarese and M. Reboiro (to be published).
[15] U. Vogl and W. Weise, Prog. Theor. Phys. **27**, 195 (1992); G. Hellstern, R. Alkofer, and H. Reinhardt, hep-ph/9706551; R. Rapp, T. Shaefer, E. V. Shuryak, and M. Velkovsky, hep-ph/9711396; M. Alford, K. Rajagopal, and F. Wilczek, hep-ph/9711395.
[16] H. B. Geyer and F. J. W. Hahne, Phys. Lett. **97B**, 173 (1980); H. B. Geyer, Phys. Lett. B **182**, 111 (1986).
[17] J. L. Armony and D. R. Bes, Phys. Rev. C **47**, 1781 (1993).
[18] J. Dukelsky and P. Schuck, Phys. Lett. B **387**, 233 (1996).
[19] J. F. Cornwell, *Group Theory in Physics*, Vol. II (Academic, New York, 1984), pp. 869–875.
[20] K. T. Hecht, Nucl. Phys. **63**, 177 (1963).
[21] O. Civitarese, P. Hess, J. Hirsch, and M. Reboiro (to be published).